Cross derivative of the Gibbs free energy: A universal and efficient method for phase transitions in classical spin models

Y. Chen [1], K. Ji [2], Z. Y. Xie [3,*] and J. F. Yu [1,†]

[1] *Department of Applied Physics, School of Physics and Electronics, Hunan University, Changsha 410082, China*
[2] *Department of Physics, Shanghai Normal University, Shanghai 200234, China*
[3] *Department of Physics, Renmin University of China, Beijing 100872, China*

(Received 14 October 2019; revised manuscript received 26 March 2020; accepted 30 March 2020; published 20 April 2020)

With an auxiliary weak external magnetic field, we reexamine the fundamental thermodynamic function, Gibbs free energy $G(T, h)$, to study phase transitions in classical spin lattice models. A cross derivative, i.e., the second-order partial derivative of $G(T, h)$ with respect to both temperature and field, is calculated to precisely locate the critical temperature, which also reveals the nature of a transition. The strategy is efficient and universal, as exemplified by the five-state clock model, two-dimensional (2D) and 3D Ising models, and the XY model, no matter if a transition is trivial or exotic with complex excitations. More importantly, other conjugate pairs could also be integrated into a similar cross derivative if necessary, which would greatly enrich our vision and means to investigate phase transitions both theoretically and experimentally.

DOI: 10.1103/PhysRevB.101.165123

I. INTRODUCTION

Phases of matter and phase transitions have always been hot topics in statistical and condensed-matter physics. For decades, Landau's symmetry-breaking theory was believed fully qualified to identify and describe different phases and phase transitions in between. As a seminal illustration of the spontaneous symmetry breaking, the classical Ising model (Z_2 symmetry) on the square lattice undergoes a typical order-disorder phase transition. Its opposite extreme, the continuous XY model [$U(1)$ symmetry], involves the exotic topological vortices excitation and a phase transition without symmetry breaking, i.e., the so-called Kosterlitz-Thouless (KT) [1,2] transition beyond Landau's theory. Both types of transitions can be easily probed by the magnetic susceptibility, which reflects the system's response to an external magnetic field and behaves distinctively across the critical point.

One natural question is how the universality class evolves with the symmetry of the models, which arouses intensive interest in the intermediate q-state clock model with a finite q. As is well known, when q is no bigger than 4, it has one unique second-order phase transition; otherwise, there are two separate transitions sandwiching a critical KT phase with quasi-long-range order. So far, major debates focus on q near 5 about the nature and universality classes of the phase transitions.

Usually, Monte Carlo (MC), one of the principal methods for many-body problems, calculates the helicity modulus [3–7] to characterize the KT transition. As in the continuous XY model on the square lattice, it jumps abruptly from finite to zero at the critical point [8]. For the five-state clock model, at the upper transition point, it behaves similarly to the XY case. However, as to the lower one, inconsistent conclusions about the transition type were claimed by different groups with MC studies [5,6]. By proposing an extended universality class theory with MC simulations, Lapilli *et al.* [3] even declared both transitions are not KT type when $q \leqslant 6$, which is supported by Ref. [9] from a Fisher zero analysis for the $q = 6$ case. A recent Fisher zero study for $q = 5, 6, 8, 10$ [10] shows that the upper transition collapses onto the zero trajectory of the KT case in the XY limit when $q \geqslant 6$, but converges differently in the $q = 5$ case, indicating a different mechanism.

Another powerful method, the renormalization group (RG), predicted two KT transitions early [11], and a recent density matrix renormalization group (DMRG) study [12] favored this assertion by calculating the helicity modulus with relatively small system sizes. The tensor network states, generalized from DMRG to higher dimensional strongly correlated systems, have developed rapidly and been widely used to investigate both the classical and the quantum systems. Among those, the tensor renormalizaton group method based on the higher-order singular value decomposition (HOTRG) [13], has been successfully applied to study the 3D Ising model [13], the Potts model [14,15], and the continuous XY model [16]. Actually, it has also been utilized to study the five-state clock model, where the magnetic susceptibility properly describes the upper phase transition, but does not work well for the lower one [17], as also presented in Fig. 1(b). Therefore, a gauge invariant factor from the fixed point tensor of the RG flow, proposed in Ref. [18], was adopted to measure the degeneracy of each phase, which also precisely estimates the critical points of the six-state clock model [19].

*qingtaoxie@ruc.edu.cn
†yujifeng@hnu.edu.cn

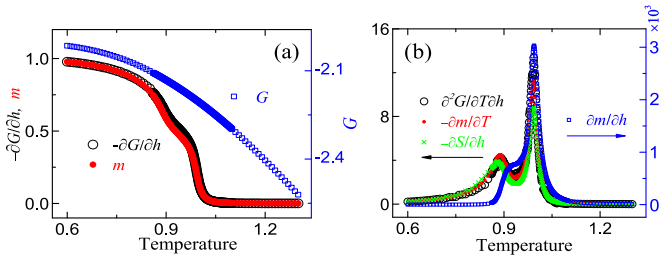

FIG. 1. (a) Gibbs free energy G (blue blank square) of five-state clock model with a magnetic field $h = 4.0 \times 10^{-5}$; comparison of $-\partial G/\partial h$ (black empty circle) and $\boldsymbol{m}$ (red filled circle); (b) magnetic susceptibility $\partial \boldsymbol{m}/\partial h$ (blue blank square), cross derivative $\partial^2 G/\partial T\partial h$ (black blank circle), $-\partial \boldsymbol{m}/\partial T$ (red filled circle), and $-\partial S/\partial h$ (green cross).

Nevertheless, some important information is still missing, e.g., the reason why the magnetic susceptibility loses its efficacy for the lower transition in this model, and the nature of the transitions in particular, although much research claimed both are KT transitions. A duality analysis by the conformal field theory (CFT) deemed that two transitions are of KT type but they still have some differences [20,21]. Recently, a universal entropy predicted by CFT on a Klein bottle [22,23] has different values at these two critical points [24], which is believed valuable to distinguish different CFTs.

Here, we intend to detect and clarify the nature/mechanism of the classical phase transitions, within a unified frame, by reexamining the fundamental thermodynamic function, Gibbs free energy G, which is intrinsically a signpost of the universal entropy increase of a spontaneous change [25], and contains information about the phase transitions. However, the free energy and its temperature derivatives, i.e., the internal energy and the specific heat, are analytically continuous without any singularity in the KT transition. So, besides the temperature, we introduce an auxiliary stimulus, a weak external magnetic field, which interacts with spin degree of freedom and provides us a convenient tool to investigate the dynamical response of the system. By detailed analyses on the cross derivative of $G(T, h)$ with respect to both temperature and field, we can easily identify and precisely locate the transition points. Moreover, since the free energy is fundamental, this idea is readily applied to any classical spin system, like Ising or XY models with trivial or exotic transitions. In other words, it is universal.

II. MODELS AND METHODS

First, we demonstrate this idea explicitly by the ferromagnetic five-state clock model with an in-plane magnetic field, whose Hamiltonian is written as

$$H = -J \sum_{\langle ij \rangle} \cos(\theta_i - \theta_j) - h \sum_i \cos\theta_i, \tag{1}$$

where $\langle ij \rangle$ means summing over all nearest neighbors. θ_i is the spin angle on lattice site i, selected from $\theta = 2\pi k/q$, $k = 0, 1, 2, \ldots, q-1$. J is the nearest coupling. h is the applied field in unit of J/μ, and μ is the magnetic moment of each spin. Both J and μ are set as 1 for convenience.

Here, we employ the HOTRG method to compute the desired physical quantities. Details about the algorithms are in Refs. [13,16,17]. Its accuracy, like other RG algorithms, is subject to the number of states kept during the RG process, labeled by the bond dimension D. Initially, it equals q, then expands exponentially along the RG process. Therefore, a truncation is necessary to ensure further steps sustainable.

The free energy $G(T, h_1)$ with field h_1 is presented in Fig. 1(a), wherein $-\partial G/\partial h$ and the magnetization $\boldsymbol{m}$ are also shown. For comparison, the quantity $-\partial G/\partial h$ is computed directly from $-[G(h_2) - G(h_1)]/(h_2 - h_1)$ by using two close field strengths, and $\boldsymbol{m}$ is calculated by the impurity tensor algorithm [13,16,17]. One can see they agree well with each other as they should. For this model, as discussed in Ref. [17], the magnetic susceptibility can clearly identify the upper phase transition, but is not so capable for the lower one. As shown in Fig. 1(b) by blue blank squares, an exponential divergence clearly labels a phase transition near $T = 1.0$. Meanwhile, a broad shoulder-shape structure emerges below, indicating something happens, but not as evident as the upper one.

Instead, the cross derivative of the free energy with respect to both temperature and field, i.e., $\partial^2 G/\partial T\partial h$, is able to characterize both transitions simultaneously. Clearly, as shown in Fig. 1(b) by black blank circles, two separate sharp peaks show up. In particular, the upper one is coincident perfectly with the susceptibility curve for both the position and the shape, although it decays exponentially from a much smaller peak other than divergence as in the magnetic susceptibility. The lower one, small but similarly obvious, locates near $T = 0.90$. Here, a relatively small bond dimension $D = 40$ is used just for illustration.

As verified in Fig. 1(a), $-\partial G/\partial h$ is just $\boldsymbol{m}$, then the cross derivative equals the temperature derivative of the magnetization $-\partial \boldsymbol{m}/\partial T$. As both shown in Fig. 1(b), they match up well with each other. Equally, one can choose function $-\partial S/\partial h$, as also presented in Fig. 1(b), because $-\partial G/\partial T$ is just the thermodynamic entropy S. Additionally, the Maxwell relation [26] $\partial S/\partial h = \partial \boldsymbol{m}/\partial T$ is numerically verified by computing S directly from the difference between Gibbs free energy and the internal energy, because both terms essentially spring from the cross derivative. For numerical simplicity and convenience, we adopt the notation $-\partial \boldsymbol{m}/\partial T$ hereafter, while keeping in mind its physical origin.

Some may question the validity or the physical meaning of this cross derivative. One can imagine slicing the 3D curved surface $G(T, h)$ along the h axis, then performing the derivative $\partial G/\partial T$ for each h slice, and observing its evolution along the h axis; or equivalently slicing $G(T, h)$ along the T axis and obtaining $\partial G/\partial h$, then investigating its evolution along the T axis. Thus, each captures the effects of both temperature and field, and the system dynamics can be easily deduced. This scheme may be elaborated by a formula

$$\left(\frac{\partial}{\partial T} + \frac{\partial}{\partial h}\right)^2 G = \nabla^2 G + 2\frac{\partial^2 G}{\partial T\partial h}, \tag{2}$$

where the left part in parentheses is a linear combination of two derivative operators in the two-dimensional orthogonal space expanded by temperature and field, and the Laplacian

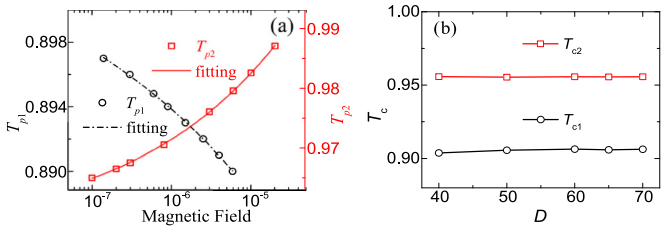

FIG. 2. (a) Illustration of the peak positions of $-\partial \boldsymbol{m}/\partial T$ versus the magnetic fields for five-state clock model with $D = 40$, along with a power-law fitting to extrapolate the transition temperature as $T_{c1} = 0.9038$ and $T_{c2} = 0.9557$, respectively; (b) The transition temperature versus the tensorial bond dimension D to obtain the converged T_c as 0.9063 and 0.9557, respectively.

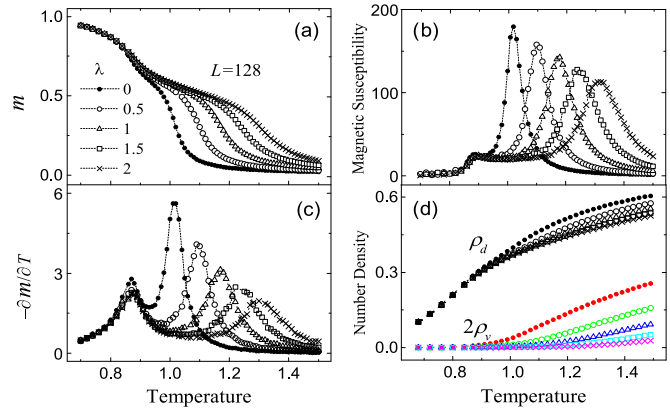

FIG. 3. MC simulation of the Hamiltonian [Eq. (3)] with $L = 128$ for different λ: (a) magnetization, (b) magnetic susceptibility, (c) $-\partial \boldsymbol{m}/\partial T$, (d) number densities of the domain walls (ρ_d) and the vortices (ρ_v), where ρ_v is multiplied by 2 for a better view.

stands for the second-order derivatives with respect to each individual parameter, i.e., the specific heat and the magnetic susceptibility, respectively, while neither is adequate to characterize the system dynamics comprehensively. We are also informed that early MC studies [27–29] used similar cross derivative quantities by applying the scaling hypothesis to determine the transition temperature and the critical exponent ν of the 3D Ising model and other models in same universality class.

III. RESULTS AND DISCUSSIONS

Similar to the procedure used in the continuous XY model to locate the transition temperature [16], we vary the applied field and obtain the peak positions of $-\partial \boldsymbol{m}/\partial T$, as presented in Fig. 2(a). To determine the critical points for a given D, an extrapolation to a zero field is performed by a power-law fitting $T_p - T_c \sim h^x$.

As demonstrated in Fig. 2(a), the results with $D = 40$ are obtained as $T_{c1} = 0.9038$ and $T_{c2} = 0.9557$. Likewise, we replicate the above process with different bond dimensions, and obtain the converged transition temperatures, i.e., $T_{c1} = 0.9063$ and $T_{c2} = 0.9557$, as shown in Fig. 2(b). Both agree well with the estimations from other research [6,12,17,30,31].

Once obtaining the critical points, we can calculate with the HOTRG method the critical exponent δ, which signifies the change of the system magnetization with the applied magnetic field at each transition point as $m \sim h^{1/\delta}$. The results are $\delta_1 = 15.81$ and $\delta_2 = 15.77$, respectively, by using the bond dimension $D = 70$. Both are consistent with the theoretical value $\delta = 15$ for the KT transition in the 2D XY model [2]. According to the results of CFT [32,33], we calculate the finite-size partition function on a torus by infinite time-evolving block decimation (iTEBD) algorithm [34] with $D = 40$ to obtain the central charge at two critical points and the sandwiched critical phase as $c = 1.04$, which indicates that both transitions belong to the same $c = 1$ CFT class. Combining c and δ together, it probably implies two KT type transitions. As also shown clearly in Fig. 2(a), the upper critical point shifts with the applied magnetic field, the stronger a field, the higher the transition temperature, similar to the XY case [16], because more heat energy is needed to overcome the additional barrier introduced by the magnetic field. However, as seen in Fig. 2(a), the lower one moves oppositely, which seems to indicate a different scenario. Besides the vortex excitation, another typical topological excitation responsible for the melting of the magnetic order in magnetic systems is the domain wall [31,35–37], which probably plays an important role in this transition.

To clarify the mechanism, we adopt the procedure of Refs. [38,39] and the references therein to investigate the influence of the vortices excitation on the phase transitions by introducing a parameter λ to adjust the vortex core energy as

$$H = -J \sum_{\langle ij \rangle} \cos(\theta_i - \theta_j) + \lambda \sum_{i'} |\omega_{i'}|, \tag{3}$$

where $\omega_{i'} = (\delta_{ba} - \delta_{cb} - \delta_{dc} - \delta_{ad})/5$, and δ_{ba} is $s_b - s_a$ wrapped in $[-1, 1]$. s_a, s_b, s_c, s_d are spins on four vertexes of a square plaquette labeled by i'.

By MC simulations for the above Hamiltonian [Eq. (3)] on a square lattice with $L = 128$, we obtain the magnetization, the magnetic susceptibility, and the deduced $-\partial \boldsymbol{m}/\partial T$ for different λ, as all shown in Fig. 3. Increasing the vortex core energy to suppress its formation, a clear shift of the upper critical point can be seen from each curve. Again, $-\partial \boldsymbol{m}/\partial T$ looks much more convincing than the magnetic susceptibility for the lower transition. More importantly, as manifested in Figs. 3(b) and 3(c), this lower temperature phase transition is barely affected by the vortex suppression, which strongly suggests it is dominated by the domain wall excitation [31,35–37]. A more intuitive illustration is presented in Fig. 3(d), i.e., the number density of each excitation, by adopting the definition in Ref. [38]. One can clearly observe that, near the lower transition point, the number density of the domain wall decreases negligibly, while the vortices are greatly suppressed even eliminated, when increasing λ.

Furthermore, we calculate the aforementioned universal entropy $\ln g$ of CFT on a Klein bottle [22] at each transition point by iTEBD algorithm with $D = 40$, because CFT asserts the two transitions in this model are KT type but with different g [24]. Our computation gives $g_1 = 3.30$ and $g_2 = 3.09$, respectively, both of which agree well with the CFT conclusion [24]. From the foregoing discussions, we can

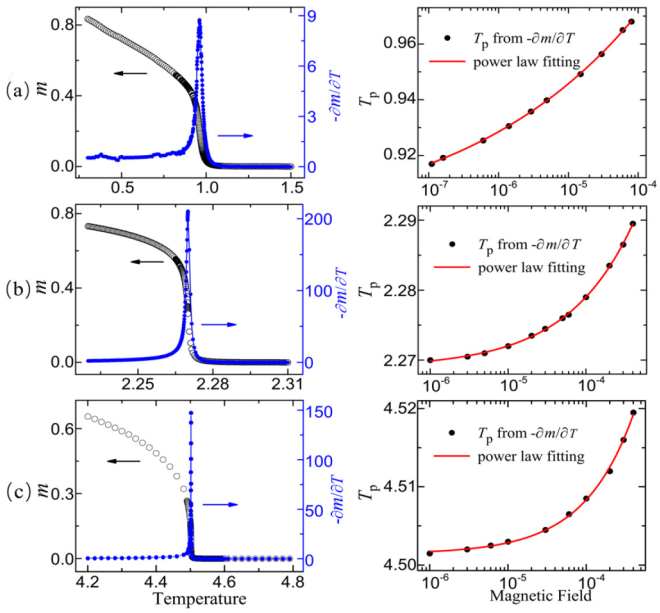

FIG. 4. $-\partial \boldsymbol{m}/\partial T$ and the power-law fitting of its peak position varying with the applied field: (a) 2D XY model with $D = 40$, (b) 2D Ising model with $D = 40$, (c) 3D Ising model with $D = 10$.

conclude that both transitions are indeed KT type, but with subtle differences: the upper one is attributed to the unbinding of the vortices pairs, while the lower one is dominated by the domain wall excitation instead; and they belong to different CFTs. The differences may be closely related to why the magnetic susceptibility works fine for the upper transition but not so well for the lower one, and why the transition points shift oppositely with the external field as shown in Fig. 2(a). They may also be the reason why studies from different groups would give controversial estimations about the nature of the transitions.

Briefly, with an auxiliary external magnetic field, the function $\partial \boldsymbol{m}/\partial T$ accurately reflects the interplay of the field and the temperature, and captures the implicit dynamics of the excitations in this model, hence correctly describing the phase transitions. While the derivative of the free energy F with respect to each single parameter, such as the specific heat or the magnetic susceptibility, is inadequate for lacking information about the internal competition/interplay among those mingled complex excitations. The auxiliary magnetic field and the cross derivative provide us a convenient way to observe the response/dynamics of different excitations.

To further check the universality of this idea, we apply it to the 2D XY, the 2D Ising, and the 3D Ising models separately. A sample of $-\partial \boldsymbol{m}/\partial T$ and the power-law fitting of the peak position for each model are illustrated in Fig. 4 as (a)–(c) respectively. For the XY case, the transition temperature is obtained at $T_c = 0.8924(16)$, which is coincident to the previous estimation [16] from the magnetic susceptibility $T_c = 0.8921(19)$ with same bond dimension $D = 40$, and both conform to the results from other methods like MC [40,41] at $T_c = 0.89294(8)$. For the 2D Ising case, the power-law extrapolation yields the transition temperature at $T_c = 2.26893(18)$, and a simultaneous prediction from the magnetic susceptibility (not shown in the figure) is $T_c = 2.26904(22)$. They agree well with each other, and with the exact value $T_c = 2/\ln(\sqrt{2}+1) \sim 2.26919$, even using a relatively small bond dimension $D = 40$. As to the 3D Ising case, the same procedure is carried out with the bond dimension $D = 10$. The similar efficiency of the function $-\partial \boldsymbol{m}/\partial T$ is clearly demonstrated once again, from which the critical temperature is located at $T_c = 4.5014(2)$. Also, the T_c is determined at 4.5013(1) from the magnetic susceptibility. Both are consistent with the prediction at $T_c = 4.5015$ by the HOTRG calculation with the same D [13]. What's more, the singularity can be clearly observed in the $-\partial \boldsymbol{m}/\partial T$ curve of the 2D/3D Ising model, indicating a second-order phase transition. It becomes sharper when lowering the field to zero and a direct determination of the critical point can be achieved without extrapolation.

IV. CONCLUSION

These examples have verified the capability of the cross derivative $\partial^2 G/\partial T \partial h$, which seems more versatile and effective, no matter if a transition is trivial or exotic, especially when multiple exotic excitations are involved and other quantities/methods are difficult to clarify. Also, we think this strategy is universal, as long as the free energy can be calculated accurately with a weak external magnetic field included. Experimentally, one can measure the system magnetization $\boldsymbol{m}(T, h)$, from which the phase transition information can be easily deduced. More importantly, the magnetic field (h) and the magnetization ($\boldsymbol{m}$) in the Gibbs free energy or the Hamiltonian are just one typical conjugate pair of generalized force and displacement [26]. Likewise, other conjugate pairs, if introduced into the Hamiltonian to regulate a system's behavior, would play a similar role in investigating the phase transitions, e.g., the electric field (E) and the polarization(p) in an electronic system, which could be similarly integrated into formula Eq. (2) as $G = U - TS - h\boldsymbol{m} + Ep + \cdots$. The case of using the electric field and polarization pair is under exploration and will be presented in subsequent reports. In such a way, we have a list or vector whose components are the partial derivatives from conjugated pairs in the Gibbs energy G. Each component can be equally effective to investigate the phase transitions. Thus, this idea will greatly enrich our vision and means to study the classical phase transitions both theoretically and experimentally.

Considering its accuracy and simplicity, the cross derivative we demonstrated in this work is efficient and universal to investigate the phase transitions in classical spin systems, trivial or complex, 2D or 3D. The predictions will be more accurate if the free energy or the physical quantities involved could be computed more precisely.

ACKNOWLEDGMENTS

We are grateful to Prof. Keiichiro Nasu, Prof. Hong-Hao Tu, Prof. Fuxiang Li, and Dr. Yu-Chin Tzeng for valuable discussions and comments. Y.C. thanks Mr. Yuan Si for help on MC simulations. This work was supported by the National Natural Science Foundation of China (No. 11974249, No. 11774420), the National R&D Program of China (No. 2016YFA0300503,

No. 2017YFA0302900), the Fundamental Research Funds for the Central Universities (No. 531107040857), the Natural Science Foundation of Hunan Province (No. 851204035), and a research foundation of Renmin University of China.

[1] J. M. Kosterlitz and D. J. Thouless, J. Phys. C **6**, 1181 (1973).
[2] J. M. Kosterlitz and D. J. Thouless, J. Phys. C **7**, 1046 (1974).
[3] C. M. Lapilli, P. Pfeifer, and C. Wexler, Phys. Rev. Lett. **96**, 140603 (2006).
[4] S. K. Baek and P. Minnhagen, Phys. Rev. E **82**, 031102 (2010).
[5] S. K. Baek, H. Mäkelä, P. Minnhagen, and B. J. Kim, Phys. Rev. E **88**, 012125 (2013).
[6] Y. Kumano, K. Hukushima, Y. Tomita, and M. Oshikawa, Phys. Rev. B **88**, 104427 (2013).
[7] T. Surungan, S. Masuda, Y. Komura, and Y. Okabe, J. Phys. A: Math. Theor. **52**, 275002 (2019).
[8] P. Minnhagen and B. J. Kim, Phys. Rev. B **67**, 172509 (2003).
[9] C.-O. Hwang, Phys. Rev. E **80**, 042103 (2009).
[10] D.-H. Kim, Phys. Rev. E **96**, 052130 (2017).
[11] J. V. José, L. P. Kadanoff, S. Kirkpatrick, and D. R. Nelson, Phys. Rev. B **16**, 1217 (1977).
[12] C. Chatelain, J. Stat. Mech. (2014) P11022.
[13] Z. Y. Xie, J. Chen, M. P. Qin, J. W. Zhu, L. P. Yang, and T. Xiang, Phys. Rev. B **86**, 045139 (2012).
[14] M. P. Qin, J. Chen, Q. N. Chen, Z. Y. Xie, X. Kong, H. H. Zhao, B. Normand, and T. Xiang, Chine. Phys. Lett. **30**, 076402 (2013).
[15] S. Wang, Z. Y. Xie, J. Chen, B. Normand, and T. Xiang, Chin. Phys. Lett. **31**, 070503 (2014).
[16] J. F. Yu, Z. Y. Xie, Y. Meurice, Y. Z. Liu, A. Denbleyker, H. Y. Zou, M. P. Qin, J. Chen, and T. Xiang, Phys. Rev. E **89**, 013308 (2014).
[17] Y. Chen, Z.-Y. Xie, and J.-F. Yu, Chin. Phys. B. **27**, 080503 (2018).
[18] Z. C. Gu and X. G. Wen, Phys. Rev. B **80**, 155131 (2009).
[19] J. Chen, H.-J. Liao, H.-D. Xie, X.-J. Han, R.-Z. Huang, S. Cheng, Z.-C. Wei, Z.-Y. Xie, and T. Xiang, Chin. Phys. Lett. **34**, 050503 (2017).
[20] S. Elitzur, R. B. Pearson, and J. Shigemitsu, Phys. Rev. D **19**, 3698 (1979).
[21] H. Matsuo and K. Nomura, J. Phys. A: Math. Gen. **39**, 2953 (2006).
[22] H.-H. Tu, Phys. Rev. Lett. **119**, 261603 (2017).
[23] W. Tang, X. C. Xie, L. Wang, and H.-H. Tu, Phys. Rev. B **99**, 115105 (2019).
[24] H.-H. Tu (private communication).
[25] P. Atkins, *The Laws of Thermodynamics: A Very Short Introduction* (Oxford University Press, Oxford, 2010).
[26] L. E. Reichl, *A Modern Course in Statistical Physics* (Wiley-VCH, Weinheim, Germany, 2016).
[27] A. M. Ferrenberg and D. P. Landau, Phys. Rev. B **44**, 5081 (1991).
[28] H. W. J. Blöte, E. Luijten, and J. R. Heringa, J. Phys. A: Math. Gen. **28**, 6289 (1995).
[29] Y. Deng and H. W. J. Blöte, Phys. Rev. E **68**, 036125 (2003).
[30] O. Borisenko, G. Cortese, R. Fiore, M. Gravina, and A. Papa, Phys. Rev. E **83**, 041120 (2011).
[31] S. Chatterjee, S. Puri, and R. Paul, Phys. Rev. E **98**, 032109 (2018).
[32] H. W. J. Blöte, J. L. Cardy, and M. P. Nightingale, Phys. Rev. Lett. **56**, 742 (1986).
[33] I. Affleck, Phys. Rev. Lett. **56**, 746 (1986).
[34] G. Vidal, Phys. Rev. Lett. **98**, 070201 (2007).
[35] G. Ortiz, E. Cobanera, and Z. Nussinov, Nucl. Phys. B **854**, 780 (2012).
[36] M. B. Einhorn, R. Savit, and E. Rabinovici, Nucl. Phys. B **170**, 16 (1980).
[37] H. A. Fertig and K. Majumdar, Ann Phys. **305**, 190 (2003).
[38] S. Bhattacharya and P. Ray, Phys. Rev. Lett. **116**, 097206 (2016).
[39] R. Zhao, C. Ding, and Y. Deng, Phys. Rev. E **97**, 052131 (2018).
[40] M. Hasenbusch and K. Pinn, J. Phys. A **30**, 63 (1997).
[41] Y. Tomita and Y. Okabe, Phys. Rev. B **65**, 184405 (2002).